

# CONVERSION FROM STOCHASTIC TO CHAOTIC APPROACH IN RESEARCH AND DESIGN

By S. Dora and J. Gedeon, D.Sc.  
Budapest University of Technology and Economics,  
Hungary

Presented to the XXVII OSTIV Seminar, Mafikeng, South Africa

## SUMMARY

A gradual conversion from stochastic to chaotic approach in the analysis of measurement records, dynamic movement and stress analysis, etc. is recommended. A practical problem with that is, that the use of mathematical laws and formulae published in chaotics requires mostly the beforehand knowledge of the appropriate differential equations, we are seldom in the possession of. To evade this difficulty an attempt is made to elaborate chaotic concepts to the analysis of chaotic records, too. Three detail problems have been picked out to start the line of applications with. Early classification of the records and control of the sampling frequency is the first candidate to begin with. A generalization of the geometric similarity concept, too, promises to give dividends. Finally, we report on the first trials to detect the true structure of chaotic spectra.

## NOTATION

F	frequency
H	sampling interval
I	sampling serial number
R	radius (polar coordinates)
R	amplitude of the Fourier component
X	the measured/recorded variable
X	horizontal co-ordinate
Y	vertical co-ordinate
Rx	autocovariance function
T	analysis base time, period
Sh	neighborhood number
Q	angle
Xx	scale of two figures
M	mean
X	standard deviation of the variable
X	displacement
X	degree of distortion
Xx	displacement in units of h
Xx	angular displacement resp. difference of angles
Xx	degree of similarity

## INTRODUCTION

In national sciences the traditional concept of deterministic laws is slowly making way for statistical methods. The final outcome of this trend was the theory of stochastic

processes (see e.g. Karin and Taylor [10], Bendat and Piersol [2,3]). Its mathematical foundations are mathematical statistics and probability theory. Aeronautical research, being always in the vanguard of fluid dynamics and dynamic stressing, had ample opportunity to analyze apparently random, non-deterministic problems. A statistical treatment of turbulence records was requisite from the outset. Based on the analogue instruments and methods then available correlation functions (i.e. statistics of products) were added to simple statistics. The palette was completed with a special variety of Fourier calculus: the spectral density function.

Stricly speaking, even the correlation function points beyond the limits of the original probability concept. Namely the autocovariance function of a true random series I theoretically zero except at the point of origin (see Fig. 1).

The spectral density function, derived from the autocovariance, is even more suspicious for not being truly covered by the original concept of the probability theory. This surmise will not mean that a practical calculation using the PSD function shall give inaccurate results, it will only draw attention to the fact that we do not know exactly at present, all its possibilities and limitations.

So the theory of turbulence has grown with and beyond the original statistical concepts. Meanwhile, a third way of thinking, the chaos theory, too, came into being. Basically it is the analysis of all the possible solutions of nonlinear differential equation systems. One of its top models is once again turbulence. Is it advisable to convert to this new concept? If so, in which provinces of aeronautical engineering? What are the benefits of the conversion and how it can be made in practice?

The chaos theory promises to give more strong laws and more exact results than the probability theory. It seems therefore worth the trouble to try the conversion. But the practical problem is that except some recent works (e.g. Abarbanel [1]) chaology is a highly theoretical way of thinking using mostly deductive procedures. The engineer, on the contrary, has and will work primarily using inductive methods, e.g. by analysis of measurement records. So the problem of conversion boils down to the correct and efficient analysis and modeling of chaotic data records. The present paper attempts to develop some new concepts and procedures in this line.

First of all, a proposal for revision of the classification of records resp. of functions will be made. The conversion to chaotic methods and procedures promises to turn into a hard and lengthy process we can give here only the first attempts of.

Early classification and rating of the sampling frequency is facilitated by use of a novel graphical representation and by a rating number. Real benefits are to be expected from a generalization of the traditional geometric similarity concept. The concept of spectral analysis seems to need revision, too, but at present it is only the starting of the research and some early particulars we can report on.

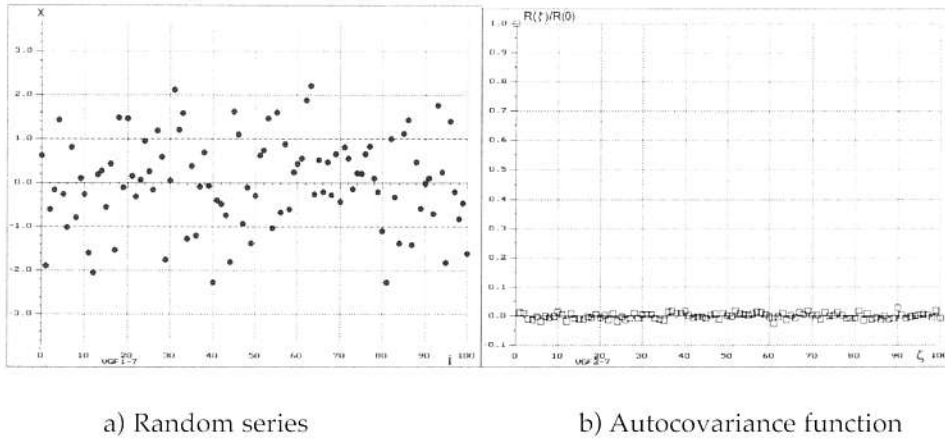


Figure 1: The beginning of a Gaussian random series and its autovariance function.

### CLASSIFICATIONS AND NEIGHBOURHOOD

In the following we shall discuss the assessment and analysis of different digital measurements records  $x_i$  ( $i=0 \rightarrow m$ ) sampling being taken in equally spaced intervals  $h$ . The examination is essentially restricted to stationary phenomena in a sense that temporarily we do not analyze the validity of the statements for nonstationary cases. According to the new approach we are working with three classes of records: the first being deterministic and the third one being the class of true random records. In between them, in the second class, there are the chaotic records as turbulence, surface elevation along the course of a rolling wheel, sea waves, etc.

Mode and extent of analysis depends to some extent on the nature, i.e. on the class, of the record. Classification made on the basis of the neighbourhood figure  $x_{i+1}=f(x_i)$  as shown in the following charts. If the sampling interval  $h$  was selected small enough, then the points sampled from a deterministic function are forming a 45° straight line as on Fig. 2a.

results in a picture similar to Fig. 2a. On the other hand the discretization by sampling introduces a peculiar kind of randomness we shall speak of later.

True random functions or records do not display any correlation or continuity; they are sequences of statistically independent measurable events (see Fig. 1). The neighbourhood figure of a uniformly distributed series looks like Fig. 4a while a Gaussian distribution gives a picture as in Fig. 4b. Several other variants, too, can be generated. Their common characteristic is symmetry for the horizontal as well as for the vertical axis.

The human eye and brain are indispensable for correct judgment but many times a suitable numerical rating, too, may give good services. It is possible to condense the essential information of the neighbourhood figure in the form of the neighbourhood number

$$\delta_h = \frac{1}{\sigma} \left[ \frac{1}{m} \sum_{i=0}^{m-1} (x_{i+1} - x_i)^2 \right]^{1/2} \quad (1)$$

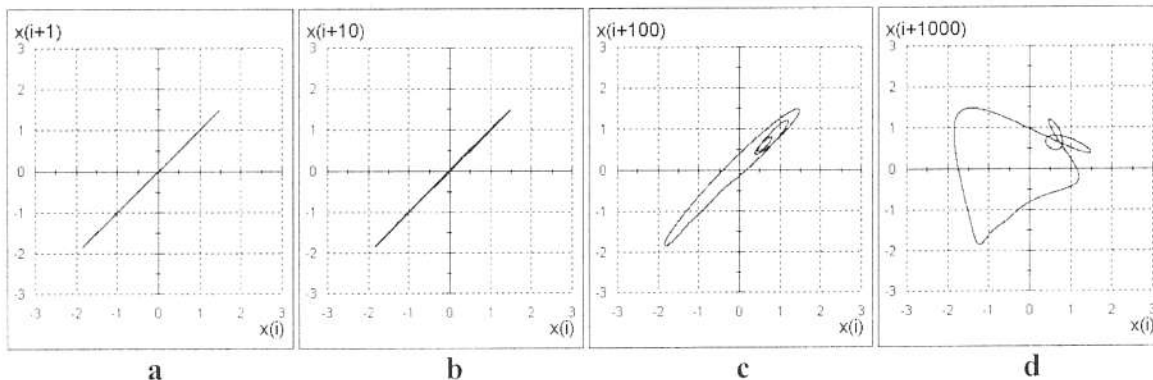


Figure 2: Neighbourhood figures of a deterministic periodic record.

Chaotic functions, if the sampling interval was short enough, as giving a more or less narrow and dense group of points along the 45° line as in Fig. 3a. Reducing the sampling interval  $h$  results in nearing the picture to this line. For every continuous function the limit procedure  $h \rightarrow 0$

Calculated from the picture, this number indicates if the sampling frequency is high enough for showing the fine details, too, of the recorded function. Both are functions of the class of the record as well as of the sampling interval  $h$ . As it can be easily shown, for all continuous records

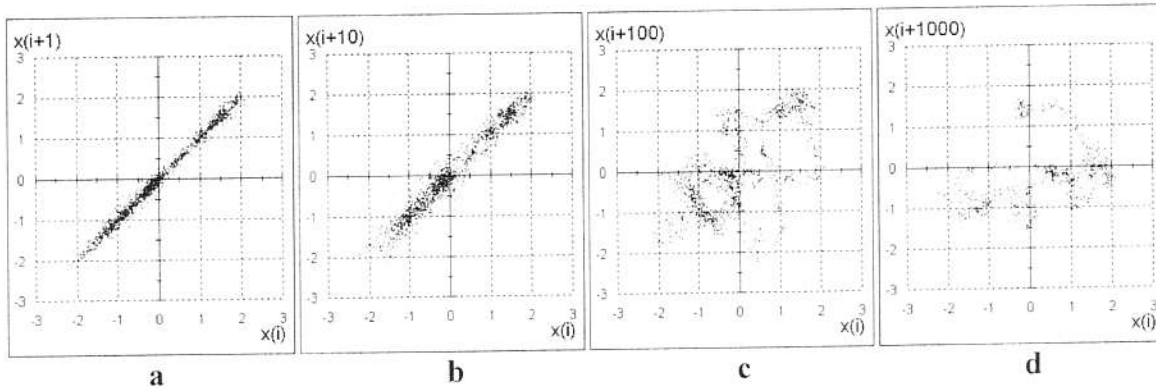


Figure 3: Neighbourhood figures of a chaotic record.

$$\lim_{h \rightarrow 0} \delta_h = 0 \quad (2)$$

Drawing of the neighbourhood figure and calculation of the neighbourhood number can be repeated doubling, trebling, etc. the sampling interval. The formula for it reads:

$$\Delta i) = \frac{1}{\sigma} \left[ \frac{1}{m - \Delta i + 1} \sum_{i=0}^{m-\Delta i} (x_{i+\Delta i} - x_i)^2 \right]^{1/2} \quad (3)$$

Fig. 2b, 2c and 2d are showing the change in the character of the neighbourhood figure of a 5 member harmonic series  $\Delta i=10, 100$  and  $1000$ , respectively. The figure remains a sharp line maybe forming some loops. Doing the same for the chaotic case (Fig. 3b, 3c and 3d) results in a scattering of the individual points (Fig. 4b, 4c and 4d) giving already for the  $\Delta i=10$  a nearly randomlike appearance. For true random series augmentation of  $\Delta i$  does not give any well-marked change.

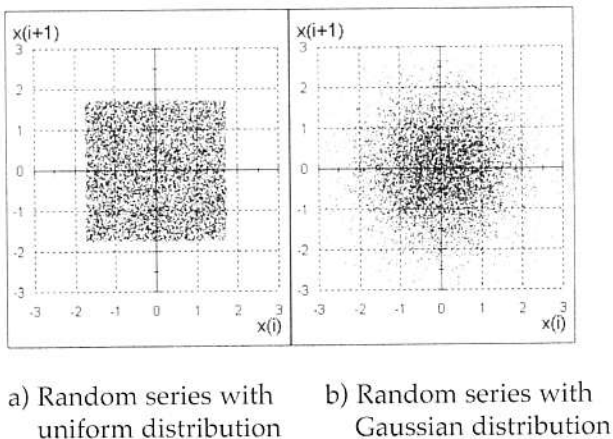


Fig. 4: Neighbourhood figures of two true random records.

Successive augmentation of  $\Delta i$  (strictly speaking of  $\Delta i.h$ ) gives the neighbourhood function, the value of the neighbourhood number as function of the time or space displacement (Fig. 5).

Deterministic periodic functions (Fig. 5a) gives  $\delta_h=0$  in intervals corresponding to their basic periods and periodic neighbourhood functions. Chaotic functions display neighbourhood functions like Fig. 5b. These start from  $\delta_h=0$  and the oscillations do not return to zero. The theoretical value of the neighbourhood number for true random functions is  $\delta_h=\sqrt{2}$  independent of the value of  $\Delta i.h$  (Fig. 5c). Some numerical values are given in Table 2.

A detailed examination of the initial trend in neighbourhood functions calculated from sampled chaotic functions reveals a peculiarity. Although the function sampled is continuous, extrapolation of the trend to  $h=0$  doesn't intersect the vertical co-ordinate axis at  $\delta_h(0)=0$  (see e.g. Fig. 6). Sampling and digitizing introduces an amount of true random errors. The value of the extrapolated  $\delta_h=0$  may therefore be weighed to be a statistical index for measuring errors. Analog records, too, aren't free of them, but continuity is masking it.

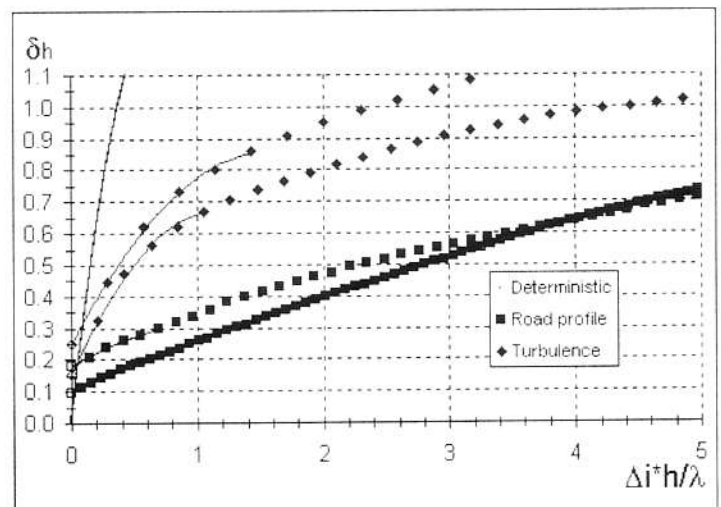


Fig. 6: Trend of the neighbourhood numbers.

The neighbourhood function can be shown (see App. 1) to possess a close relationship to the autocovariance function  $R_x(\Delta i, h)$ . It reads:

$$\delta_{\Delta i, h} = \sqrt{2} \left[ 1 - \frac{R_x(\Delta i, h)}{\sigma_x^2} \right]^{1/2} = \sqrt{2} \left[ 1 - \frac{R_x(\Delta i, h)}{R_x(0)} \right]^{1/2} \quad (4)$$

Systematic measurements are indispensable for progress in design and in practical soaring. Digitally sampled flight or wind-tunnel measurement records always contain random error components being statistically constant irrespective of the sampling interval  $h$ . A check using the neighbourhood method is recommended in all such cases.

This concept can be developed for two-dimensional observation networks, e.g. meteorological stations, showing if the number of stations is enough and their placing is correct for monitoring a given parameter of the weather. Any integer displacement  $\Delta i$  is principally a sample taken from a continuous real displacement  $\zeta = \Delta i \cdot h$ . This way a plane or spatial set of sample points can be processed like a scalar problem.

ures an extension of the definition and a suitable index number for ranking is recommended. The concept is defined and a recommended procedure is presented first for polygons and then for curvilinear plane forms.

### Polygons

A necessary requirement for the similarity of two polygons, as  $a$  and  $b$  on Fig. 7a, is the similarity of their respective characters. In other terms: the number and sequence of the discrete elements (angles and sides) should be the same and the ratio of the proportion of their greatest to their smallest dimension should not be greatly different.

If these primary conditions are performed then the similarity can be rated as shown on the case of hexagons  $a$  and  $b$  on Fig. 7 (Gedeon[9]). The procedure starts with the calculation of the respective central points  $0$ . Measured from the central points the position vectors of the corner points are given in terms of polar coordinates:

$$\mathbf{r}_{ai} = |\mathbf{r}_{ai}| e^{j\varphi_{ai}} \quad \text{and} \quad \mathbf{r}_{bi} = |\mathbf{r}_{bi}| e^{j\varphi_{bi}}$$

Table 1: Classification of records resp. of functions

Class:	Autocovariance function (if any):	Neighbourhood figure:	Neighbourhood number:
Deterministic	Constant amplitude	Sharp	$\lim_{\Delta i \rightarrow 0} \delta_h(\Delta i) = 0$
Chaotic	$\lim_{\zeta \rightarrow \infty} R_x(\zeta) = 0$	More or less diffuse	$\lim_{\Delta i \rightarrow 0} \delta_h(\Delta i) = 0$
True random	$\zeta > 0: R_x(\zeta) = 0$	Points all over the picture	$\delta_h = \sqrt{2}$

Table 2: Value of neighbourhood number of functions

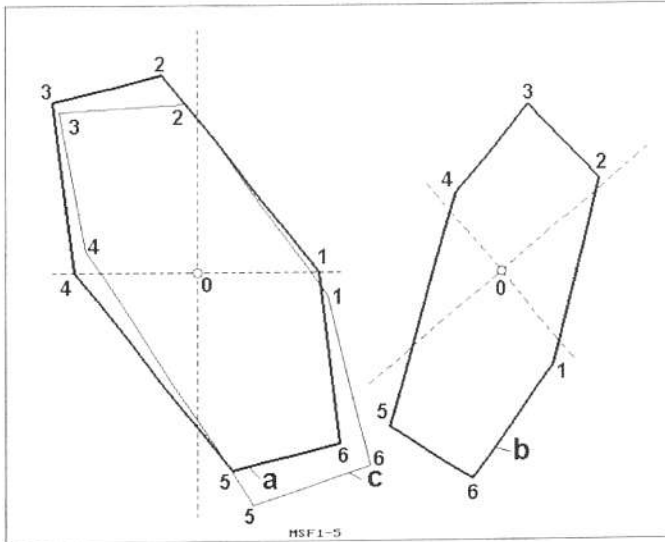
Class:	$\Delta i =$				
	1	3	10	100	1000
Deterministic	0,0015	0,0044	0,0145	0,1448	1,1247
Chaotic	0,1107	0,1412	0,2230	0,9128	1,2719
Random (Uniform)	1,4245	1,4126	1,4136	1,4173	1,4219
Random (Gaussian)	1,4058	1,4214	1,4035	1,4182	1,4048

### GEOMETRICAL SIMILARITY

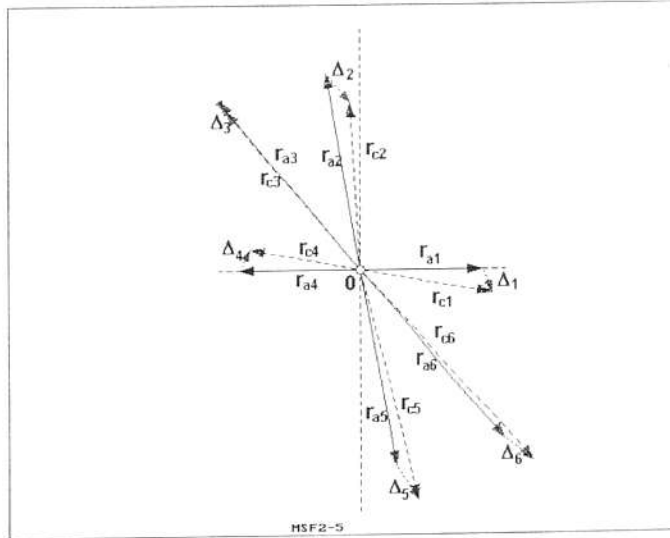
Progress in research and development is sometimes due to the recognition of similarity. It is desirable to transfer this as far as possible from human insight to numerical methods. The traditional Euclidean similarity definition accepts only full similarity giving perfect coincidence after transformations. Being this not achievable for chaotic fig-  
**TECHNICAL SOARING**

The size of the polygons should be the mean of the norms:

$$\mu_a = \frac{1}{m} \sum_{i=1}^m |\mathbf{r}_{ai}| \quad \text{and} \quad \mu_b = \frac{1}{m} \sum_{i=1}^m |\mathbf{r}_{bi}| \quad (5)$$



a) The polygons



b) Vector diagram for error calculation

Fig. 7: Calculation of the similarity index for polygons.

The scale of the two polygons is:

$$\lambda_{ba} = \frac{\mu_a}{\mu_b} \quad (6)$$

The average of the difference of corner angles gives the degree of turning:

$$\Delta\varphi = \frac{1}{m} \sum_{i=1}^m (\varphi_{bi} - \varphi_{ai}) \quad (7)$$

For the similarity calculations polygon b is taken to be displaced, turned and magnified or diminished from polygon a. For the rating this conceptual process is reversed giving hexagon c. Strictly speaking the similarity calculation

is comparison of figures a and c.

The scale of distortion can be declared in terms of Cartesian co-ordinates as shown in Fig. 7b:

$$\Delta_{ba} = \left\{ \frac{1}{m} \sum_{i=1}^m \left[ \left( \frac{\lambda_{ba} x_{bi} - x_{ai}}{\mu_a} \right)^2 + \left( \frac{\lambda_{ba} y_{bi} - y_{ai}}{\mu_a} \right)^2 \right] \right\}^{1/2} \quad (8)$$

The scale of similarity can be written alike as:

$$\Lambda_{ba} = \left\{ \frac{1}{m} \sum_{i=1}^m \left[ 1 - \left( \frac{\lambda_{ba} x_{bi} - x_{ai}}{\mu_a} \right)^2 - \left( \frac{\lambda_{ba} y_{bi} - y_{ai}}{\mu_a} \right)^2 \right] \right\}^{1/2} \quad (9)$$

For the hexagons a and b on Fig. These formulae gave a distortion of  $\Delta_{ba}=0.1725$  and a similarity number of  $\Lambda_{ba}=0.9850$  respectively.

### Curvilinear plane figures

A possible procedure, the integral method for similarity ranking, is made as follows (Gedeon [8,9]). First of all a suitably and equally situated central point 0 (e.g. the CM) on both forms a and b should be marked as shown on Fig. 8. Then starting from a base direction the shape function  $r(\varphi)$  for both forms is recorded (right square on Fig).

Integration of both functions gives the mean radius values  $\mu_a, \mu_b$  and their ratio  $\lambda_{ba}$ :

$$\mu_a = \frac{1}{2\pi} \int_0^{2\pi} r_a(\varphi) d\varphi \quad \mu_b = \frac{1}{2\pi} \int_0^{2\pi} r_b(\varphi) d\varphi \quad (10)$$

$$\lambda_{ba} = \frac{\mu_a}{\mu_b} \quad (11)$$

Marking characteristic points on the records is giving:

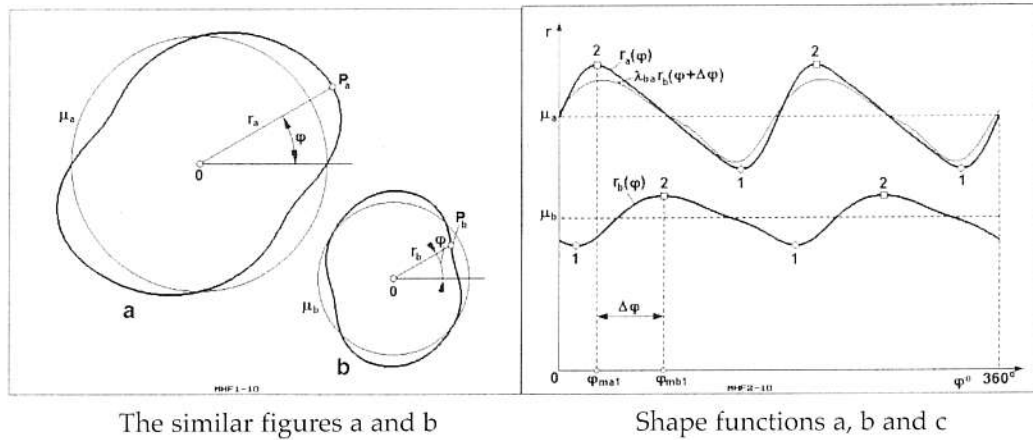
$$\Delta\varphi = \varphi_{mb} - \varphi_{ma} \quad (12)$$

The transformed curve for direct comparison reads:

$$r_c(\varphi) = \lambda_{ba} r_b(\varphi + \Delta\varphi) \quad (13)$$

On these lines the scale of distortion can be calculated to be:

$$\Delta_{ba} = \left[ \frac{1}{2\pi} \int_0^{2\pi} \left( \frac{\lambda_{ba} r_b(\varphi + \Delta\varphi) - r_a(\varphi)}{\mu_a} \right)^2 d\varphi \right]^{1/2} \quad (14)$$



The similar figures a and b

Shape functions a, b and c

Figure 8: Calculation of the similarity index by the integral method.

Using it a possible rating formula is:

$$\Lambda_{ba} = \left\{ \frac{1}{2\pi} \int_0^{2\pi} \left[ 1 - \left( \frac{\lambda_{ba} r_b(\varphi + \Delta\varphi) - r_a(\varphi)}{\mu_a} \right)^2 \right] d\varphi \right\}^{1/2} \quad (15)$$

For the two forms on Fig. 8 the distortion is  $\Delta_{ba}=0.0325$  and the similarity  $\Lambda_{ba}=0.9951$  respectively.

Comparison of spatial formations can be treated similarly extending the calculation procedures to three dimensions. Practical application of the similarity calculations may be for control of manufacturing tolerances (e.g. wind-tunnel models, sailplane wing profiles) for comparison of spectra, etc. Last but not least, it can give us a fine tool for control of canopy distortions affecting flight safety. A double-exposure picture of an orthogonal screen directly and through the canopy will show and rate any irregularities affecting the vision of the pilot. Structural integrity of fiber-reinforced sailplane structures can be checked using e.g. pulsed laser double exposure holography (fagot et al. Ref. [4])

### SPECTRAL ANALYSIS AND PHASE SPACE RECONSTRUCTION

Spectral analysis is indispensable for examination and modeling of stochastic/chaotic phenomena or shapes. After a lengthy debate the Fourier calculus was accepted for the analysis of periodic records in science and engineering. Later a similar procedure for stochastic records, too, was requested. These functions aren't periodic. This difficulty was solved by replacing the Fourier series by the spectral density function, Fourier transform of the autocovariance function.

The solution seemed to work as expected, giving acceptable input-output relations. Declaring a harmonic series  $G_x(f)$  - e.g. a Fourier series or a similar function - to be the spectrum of a function  $x=x(t)$  has strictly speaking a duplicate meaning. First it will mean that the (infinite) sum

of the series approximates the value of the function exactly and uniformly.

But on the other hand, if  $x(t)$  is representing a physical process, it may mean also that this movement or form was compiled from harmonic components  $G_x(f)$ . In the former sense a function may have several acceptable spectra while the later conclusion is obviously unique. Formal variations are several FFT procedures (see e.g. Bendat et Piersol [2] subchapter 9.3) as well as the complex spectral vector grouping of multiple inputs (Gedeon [5]). The case of "natural" or "structural" spectrum components is much more problematic.

Formal proof of the Fourier series calculation assumes the function  $x(t)$  to be periodic, in other words, the period  $T$  to be known. This is a necessary clause because the numerical integration gives correct values only for full period  $T$ . In theory the spectral density function  $G_x(f)$  should be continuous. In this case the spectrum value calculated using any base length  $T$  appropriate for the required frequency  $f$  is got to be exact. Because of the presumed continuity decreasing of the frequency steps  $f_{i+1}/f_i$  should result in decreasing the scattering between successive spectrum amplitudes.

This smoothing tendency failed to materialize in our practice. The sequence of road unevenness, atmospheric turbulence, etc. spectrum points is showing an excessive scatter. This aroused doubts about the continuity of stochastic/chaotic spectra. Namely it is easy to prove that incorrect base length can result in incorrect or even in totally false spectrum values simulating continuous spectra.

On Fig. 9a the function to be analysed has been composed of 5 components  $r_1-r_5$  as shown in solid lines on Fig. 9b giving a period  $T$ . If a false base frequency  $f^*=0.84f$  giving a base length  $T^*$  for the Fourier calculus is chosen, the resulting incorrect components will be  $r_1^*-r_5^*$  shown in dotted lines. Moreover, if requested, any number of fully false "components" in this case  $r_6^*-R_9^*$  too, can be produced. With this possibility in mind, the senior author tried to compute a possible discrete amplitude spectrum for

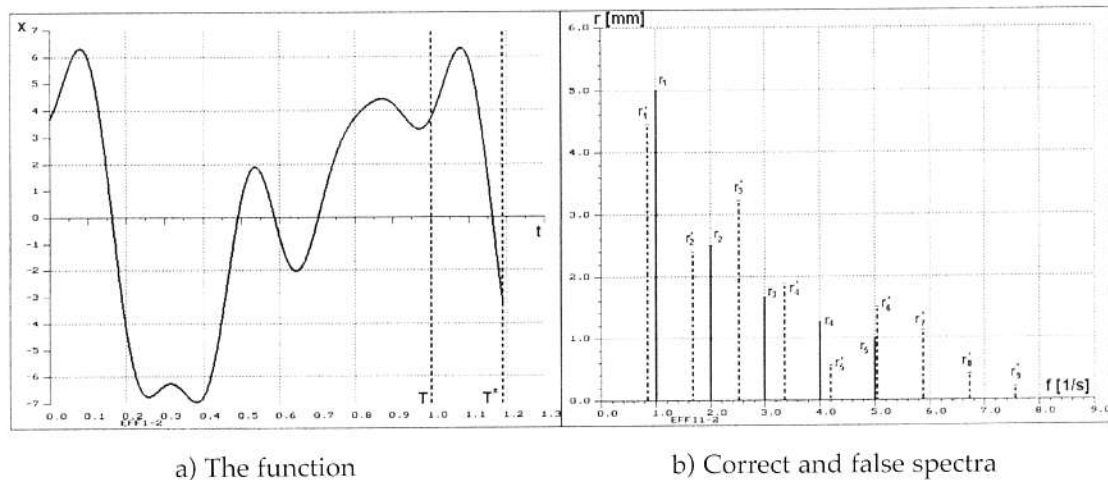


Fig. 9: False Fourier components owing to inaccurate base frequency.

four atmospheric turbulence records (Gedeon [7,8]). The experimental calculation method gave peculiar discrete-frequency amplitude spectra. Accuracy of the standard deviation as calculated from the spectra was slightly inferior to the classic method. In view of the full novelty of the problem and of some practical requirements the results could be rated to be acceptable, but there is still much to be done for getting a final and universal answer to the problem. We have to look for discrete-frequency amplitude spectra trying to find other methods, too.

Further research is going on in this line. Chaotics is working efficiently with attractors in phase spaces. They are useful for input-output calculations and perhaps they may help in the basic analysis of the spectrum structure. With that object the feasibility of a direct phase portrait calculation from chaotic records, too, is under investigation. The phase portrait could show if the spectrum can be supposed to be stationary or not. Basic improvements in the modeling of turbulence, road/terrain profile, etc. could come from this. Good ideas would be welcomed in this line.

Declaring a harmonic series  $G_X(f)$  - e.g. a Fourier series or a similar continuous function - to be "the spectrum" of a function  $x=x(t)$  has strictly speaking a duplicate meaning. First it will mean that the (infinite) sum of the harmonic series approximates the function exactly and smoothly. But, on the other hand, if  $x(t)$  is representing a physical process, it has also the second meaning that the movement or form has been induced by harmonic inputs  $G_X(f)$ . In the former sense the spectrum isn't exclusive, there may exist several acceptable solutions.

The introduction of particular discrete frequency amplitude spectra - or maybe something similar - promises to give more exact models requiring less calculations, but otherwise traditional spectral density function input-output calculations are giving acceptable results. While the spectrum structure problem waits its settling it may be safely used for a working hypothesis.

## CONCLUSIONS

Chaotics promises to open up new prospects to research and development. Conversion to the new approach is kept back by the insufficiency of chaotic record analysis procedures. In order to fill this gap development of some assessment and evaluation procedures has been initiated. Introduction of the neighbourhood calculation assures early classification of the record and checking of the sampling interval. Revision of the Euclidean similarity requirements and introduction of a ranking number promises to give help in the recognition of relations.

## ACKNOWLEDGEMENTS

The research reported herein has been sponsored in part by the Orszogos Tudományos Kutatási Alap (OTKA) under the research grant T 034537. Acknowledgements are due to Prof. Lajos Laib, Prof. Lajos Tamas and senior lecturer Zsuzsanna Szepesi for road profile resp. for wind-tunnel turbulence records.

## REFERENCES

1. Abarbaanel, H.D.I.: Analysis of Observed Chaotic Data (Springer-Verlag, New York, Berlin; 1995).
2. Bendat, J.S., Piersol, A.G.: Random Data: Analysis and Measurement Procedures (Wiley-Interscience, New York; 1971).
3. Bendat, J.S., Piersol, A.G.: Engineering Applications of Correlation and Spectral Analysis (Wiley-Interscience, New York; 1980).
4. Fagot, H., Albe, F., Smigielski, P., Arnaud, J.L.: Holographic Non-Destructive Testing of Materials Using Pulsed Lasers (Prof. 12th Congress of ICAS; ICAS-80-17.2; Munich, 1980; pp. 626-633).
5. Gedeon, J.: On the Fine Structure of Atmospheric Turbulence. Measurement, Piloting, Fatigue Tests (Technical Soaring Vol. XIV, No. 3: July 1990; pp. 89-96).

6. Gedeon, J.: Analysis of Low-Level Atmospheric Turbulence. A Case Study (Proceedings of the 6th Mini Conference on Vehicle System Dynamics, Identification and Anomalies; Budapest, 1998; pp. 503-511).

7. Gedeon, J.:

$$\delta_h(\Delta i) = \frac{1}{\sigma} \left[ \frac{1}{m - \Delta i + 1} \sum_{i=0}^{m-\Delta i} (x_{i+\Delta i} - x_i)^2 \right]^{1/2}$$

$$R_x(\Delta i, h) = \lim_{m \rightarrow \infty} \frac{1}{m - \Delta i + 1} \sum_{i=0}^{m-\Delta i} x_i x_{i+\Delta i}$$

As it is known:

$$(x_{i+\Delta i} - x_i)^2 = x_{i+\Delta i}^2 - 2x_{i+\Delta i}x_i + x_i^2$$

In addition:

$$\lim_{m \rightarrow \infty} \frac{1}{m - \Delta i + 1} \sum_{i=0}^{m-\Delta i} x_i^2 = \sigma_x^2$$

$$\lim_{m \rightarrow \infty} \frac{1}{m - \Delta i + 1} \sum_{i=0}^{m-\Delta i} x_{i+\Delta i}^2 = \sigma_x^2$$

and

$$\lim_{m \rightarrow \infty} \frac{1}{m - \Delta i + 1} \sum_{i=0}^{m-\Delta i} x_i x_{i+\Delta i} = R_x(\Delta i, h)$$

After substitution and arrangement the outcome reads:

$$\delta_{\Delta i, h} = \sqrt{2} \left[ 1 - \frac{R_x(\Delta i, h)}{\sigma_x^2} \right]^{1/2} = \sqrt{2} \left[ 1 - \frac{R_x(\Delta i, h)}{R_x(0)} \right]^{1/2}$$